Simultaneous analysis of the LFP and spiking activity reveals essential components of a visuomotor transformation in the frontal eye field

Naveen Sendhilnathan[a,b,1], Debaleena Basu[b], and Aditya Murthy[b,2]

[a]Undergraduate Programme, Indian Institute of Science, Bangalore, Karnataka 560012, India; and [b]Centre for Neuroscience, Indian Institute of Science, Bangalore, Karnataka 560012, India

The frontal eye field (FEF) is a key brain region to study visuomotor transformations because the primary input to FEF is visual in nature, whereas its output reflects the planning of behaviorally relevant saccadic eye movements. In this study, we used a memory-guided saccade task to temporally dissociate the visual epoch from the saccadic epoch through a delay epoch, and used the local field potential (LFP) along with simultaneously recorded spike data to study the visuomotor transformation process. We showed that visual latency of the LFP preceded spiking activity in the visual epoch, whereas spiking activity preceded LFP activity in the saccade epoch. We also found a spatially tuned elevation in gamma band activity (30–70 Hz), but not in the corresponding spiking activity, only during the delay epoch, whose activity predicted saccade reaction times and the cells' saccade tuning. In contrast, beta band activity (13–30 Hz) showed a nonspatially selective suppression during the saccade epoch. Taken together, these results suggest that motor plans leading to saccades may be generated internally within the FEF from local activity represented by gamma activity.

oscillations | saccades | oculomotor | frontal cortex | sensorimotor

The process of generating a motor plan from visual information entails a visuomotor transformation. The frontal eye field (FEF) is one of the cortical regions that contributes to the visuomotor transformation process by participating in critical events such as target selection (1–3) and saccade preparation (4–6). In addition to FEF, other oculomotor areas such as the lateral intraparietal cortex (7), the supplementary eye fields (8), the superior colliculus (9), and the dorsolateral prefrontal cortex (10) also possess neurons with similar properties as FEF neurons. Thus, a central question that remains unresolved is to what extent do the response properties of FEF neurons represent a cause versus a consequence of computations occurring elsewhere.

One approach to resolve this question of causation versus consequence, in the context of target selection, was the use of simultaneously recorded local field potentials (LFP) and spikes—making use of the idea that the LFP represents synchronized input coming into a brain area, as opposed to spiking activity, which is thought to represent output (11–15). Using this approach, Monosov et al. showed that FEF received spatially nonselective input through LFP earlier than spikes in the early visual epoch; however, in the consequent target selection epoch, spiking activity of FEF neurons evolved spatial selectivity and actively discriminated between the behaviorally relevant and the irrelevant stimuli earlier than the LFP (1). Such a temporal relationship between LFP and spikes during target selection in FEF has also been studied by others using simultaneously recorded LFP and spikes, converging to the same evidence (5, 16). However, whereas these studies suggest a causal role for FEF in visual selection, the causal role of FEF in saccade preparation has not yet been reported. In this study, we asked whether saccade related signals observed in FEF neurons were also generated internally or whether they represent a readout of the information brought in by other oculomotor areas. To answer this question, a temporal dissociation between visual and saccade events was necessary to analyze the signals in both epochs individually and, hence, we used a memory-guided saccade task.

Whereas simultaneous recording of spikes and LFP provide a useful approach to study input-output transformations (15), the frequency component of the LFP can also provide a complimentary approach to characterize the nature of transformations. Specifically, the role of gamma band activity (30–70 Hz) in the cerebral cortex has been a critical topic of discussion over the past decade because its activity has been correlated with cognitive roles such as attentional load (17–19), perceptual processes (20), and memory (21, 22). While the timing of gamma activity and its tuning properties make it a plausible candidate in mediating sensory-motor integration processes (23, 24), the link between saccade planning and gamma activity in FEF, is still unclear. In addition to gamma band activity, low frequency beta band (13–30 Hz) activity is also thought to play a role during movement preparation and execution (25). Beta activity is usually suppressed before a voluntary movement, gradually decreasing to reach a minima at the time of movement execution, followed by a phasic rebound (26, 27). Therefore, we also studied the relative contributions of different components of the LFP to understand their potential roles in the visuomotor transformation process within FEF.

Significance

Converting a visual input into a motor output is a fundamental computation that nervous systems have evolved to perform. In the context of saccadic eye movements, several brain areas have been identified that exhibit the effect of visuomotor computations. Nevertheless, because of dense interconnectivity between these areas, the contribution of a particular brain area to the visuomotor transformation process has not been clarified. By simultaneously recording from the local field potential (LFP) that is thought to reflect input to an area, and spiking activity that reflects its output activity, we showed that frontal eye field neurons perform the necessary visuomotor transformation to generate a saccade plan internally. We also identify specific components of the LFP such as gamma oscillations that may enable such a visual-to-motor transformation.
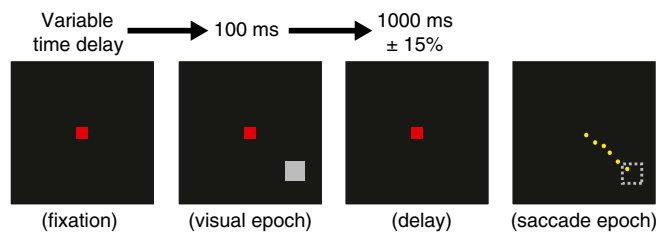
www.manaraa.com

Fig. 1. Memory-guided saccade task. The monkey fixated on a central (0.6° x 0.6°) red square fixation point on a dark background. Following a variable time delay, a peripheral gray target (1° x 1°) appeared on one of eight equally spaced positions on an imaginary circle of eccentricity 12°. The target was extinguished after 100 ms of its appearance. The monkey continued to fixate on the central fixation point for 1,000 ms (±15% jitter). When the central fixation spot was extinguished, the monkey made a single saccade (yellow trace) to the remembered target location (shown as an unfilled dashed gray square).

Results

To compare the timing of visual and saccadic responses in the LFP and simultaneously recorded spikes, we trained two macaque monkeys to perform a memory-guided saccade task, to dissociate the visual and saccadic epochs (*SI Materials and Methods* and Fig. 1). Fig. 2 shows an example neural signal and simultaneously recorded LFP in one representative site having both visual and saccadic responses as a function of eight stimulus/saccade positions. The sensory-motor responses seen in both LFP and spikes were also spatially tuned (Fig. 2, *Inset*).

Comparison of LFP and Spike Timing in the Visual Epoch. In the first stage of a saccade plan, FEF receives visual information as an input from many brain regions through the dorsal and the ventral pathways. Earlier studies have shown that the LFP signals in FEF have visual response latencies (VRLs) significantly earlier than spikes, suggesting that the LFP reflected the visual input to FEF (1, 5). In this study, we first investigated the temporal relationship between the LFP and spikes in the visual epoch to confirm this result.

We calculated the VRL of LFP and spikes by performing a *t* test between the baseline and the signals in the visual epoch (*SI Materials and Methods*). Fig. S1 shows the result of this analysis for an example LFP site (Fig. S1*A*) and a simultaneously recorded neuron (Fig. S1*B*). For all 66 recorded sites, we found that the LFP showed VRL earlier than spikes ($n = 66; P < 10^{-17}$), albeit with different latency differences between them. The VRL for the population of recorded LFP sites was 58.9 ± 1.6 ms and that of the spikes was 78.4 ± 1.2 ms. The mean difference between LFP and spike VRL was -19.5 ± 1.4 ms (Fig. S1*C*). This result suggests that the LFP has information regarding the location of the visual stimulus significantly earlier than the spikes in FEF, supporting previous studies (1, 28).

Comparison of LFP and Spike Timing in the Saccade Epoch. We calculated the time of saccade plan onset (SPO) as the first point before the start of the saccade when the signal (LFP/spike) differed from baseline (*SI Materials and Methods*). Fig. 3 shows the result of this analysis for an example (Fig. 3*A*) and the simultaneously recorded LFP (Fig. 3*B*). The SPO_{SPK} was significantly earlier than the SPO_{LFP} ($n = 66; P < 10^{-21}$) in all the sessions. Also, whereas the SPO_{SPK} showed a distributed range spanning a significant amount of the presaccadic epoch, the SPO_{LFP} was distributed in a narrow epoch close to the start of the saccade. The mean SPO_{SPK} for the population was -215.0 ± 7.0 ms and the mean SPO_{LFP} was -84.4 ± 5.6 ms before the start of the saccade, with a mean difference (ΔSPO) of -130.6 ± 9.0 ms (Fig. 3*C*).

We also calculated the saccade plan specification (SPS) time as the first time point before the start of the saccade when the signals (LFP/spikes) in at least one of the eight spatial positions differed from others (*SI Materials and Methods*). Fig. 4 shows the result of this analysis for an example neuron (Fig. 4*A*) and simultaneously recorded LFP (Fig. 4*B*). SPS_{SPK} was earlier than SPS_{LFP} for all the sessions. For the population, the mean SPS_{SPK} was -141.9 ± 6.2 ms and the mean SPS_{LFP} was 3.2 ± 4.7 ms before the start of the saccade, with a difference (ΔSPS) of -145.1 ± 8.0 ms (Fig. 4*C*).

SPS_{SPK} and SPS_{LFP} showed a similar trend as the SPO_{SPK} and SPO_{LFP} times, but shifted in time (Fig. 5*A*). The LFP showed an onset only 57.5 ± 8.3 ms after the spikes specified the saccade plan. Spikes specified the saccade direction approximately 73.1 ± 5.0 ms after they showed onset and the LFP specified the saccade direction approximately 87.6 ± 4.6 ms after their onset, suggesting that the spikes took less time to specify the saccade direction after their onset compared with the LFP ($P = 0.0148$; Fig. 5 *B* and *C*).

Furthermore, the SPO_{SPK} correlated with the SPS_{SPK} ($r^2 = 0.7166; P < 10^{-11}$) and so did their LFP counterparts ($r^2 = 0.6046; P < 10^{-8}$); however, and more importantly, the $SPO_{SPK} - SPS_{SPK}$ latency did not correlate with the $SPO_{LFP} - SPS_{LFP}$ latency ($r^2 = 0.134; P = 0.2830$). Further, neither the SPO_{SPK} correlated with the SPO_{LFP} ($r^2 = 0.036; P = 0.9771$) nor was the SPS_{SPK} correlated with the SPS_{LFP} ($r^2 = -0.0526; P = 0.6747$). Finally, the SPO_{LFP} did not correlate with the SPS_{SPK} either ($r^2 = 0.0357; P = 0.7760$), suggesting completely different origins for spikes and LFP in the saccade epoch (Fig. 5*D*). Taken together, these results suggest that in the saccade epoch, the plan for onset of saccade and the direction of saccade is specified in spikes significantly earlier than, and independent of, the LFP. We return to this point in our discussion where we suggest possible explanations for our observation.

Characterization of Gamma Band Activity in FEF. We investigated the functional role of two prominent frequency components of LFP, the gamma and the beta bands, in the visuomotor transformation process in FEF. The frequency domain information in the LFP
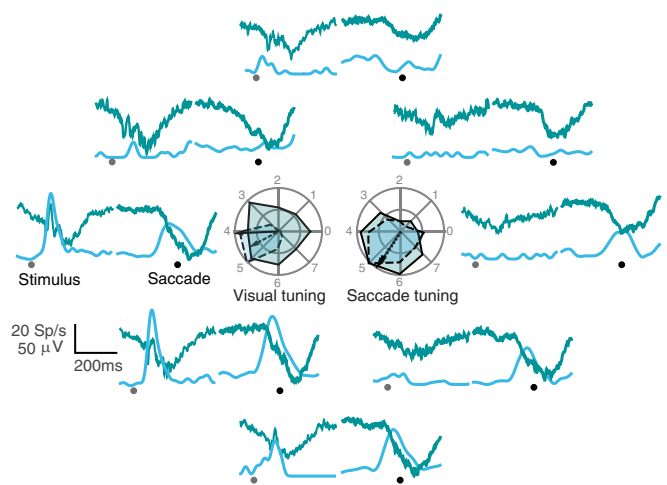

Fig. 2. Representative LFP signal and simultaneously recorded neural spikes. Average LFP (green) and spike density functions (blue) from a representative recording site for all eight stimulus locations. The first epoch shows the signals aligned to stimulus onset (gray dot), and the second epoch shows the signals aligned to saccade onset (black dot). The tuning and the preferred direction of the LFP (solid line) and the spike averaged activity (dashed line) for both stimulus and saccade epochs in all eight positions are shown in the *Inset*.
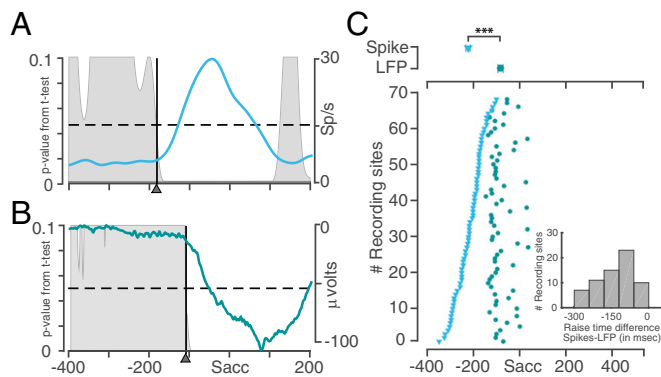
NEUROSCIENCE

Sendhilnathan et al.

Fig. 3. Saccade plan onset times for spikes and LFP. (*A*) SPO for a representative neuron. The average spike density function across all eight positions for the representative neuron (solid line) superimposed on the *P* value obtained from performing a *t* test indicating the probability that the signal was not different from the baseline (gray shaded region). The SPO for this neuron was −182 ms (vertical solid line). (*B*) SPO for the simultaneously recorded LFP signal. Same format as above. The SPO$_{LFP}$ for this site was −107 ms (vertical solid line). (*C*) (*Bottom*) SPO$_{SPK}$ (blue triangles) and SPO$_{LFP}$ (green circles) for all sessions sorted by SPO$_{SPK}$ times. *Upper* shows the mean SPO$_{SPK}$ and SPO$_{LFP}$; *t* test, *P* < 10^{-21}. *Inset* shows the distribution of ΔSPO between each SPK-LFP pair.

signal was retrieved by using a Multi Taper analysis to obtain the power of each frequency component as a function of time (*SI Materials and Methods*). Fig. 6 shows a time-frequency spectrogram constructed from a representative LFP recording signal. The gamma power was spatially tuned in the delay period (Fig. S2) and showed elevated activity in the receptive field (RF) position (Fig. 6*A*, *Left*) which sustained in the delay period and returned to baseline in the saccadic epoch (Fig. 6*A*, *Right*). This effect, while still present, was less prevalent in the antireceptive field (aRF) position (Fig. 6*B*).

Fig. 7*A* shows average z-scored gamma power as a function of time in the RF and aRF positions for the representative LFP site. Gamma showed a significant elevation in activity from baseline (0.03 ± 0.03) only in the delay epoch (0.29 ± 0.06; *n* = 58, *P* = 0.001), after which it returned to the baseline and, hence, showed no significant modulation in the saccadic epoch (−0.20 ± 0.09; *P* = 0.129; Fig. 7*B*). The gamma activity was also spatially tuned in the delay epoch (RF: 0.44 ± 0.07, aRF: 0.15 ± 0.06; *P* = 0.01; Fig. 7*C*). Interestingly, although the rise time for gamma, from the baseline, in RF was significantly earlier than in aRF (RF: 143.2 ± 13.9 ms, aRF: 233.8 ± 18.9 ms; *P* = 0.008), the peak time was comparable (RF: 257.7 ± 6.6 ms, aRF: 243.9 ± 7.9 ms; *P* = 0.402). Hence, the time when gamma differed between RF and aRF (154.3 ± 17.3 ms) was close to the gamma rise time in the RF position (Fig. 7*D*).

The above results characterize gamma activity as a spatially modulated oscillation in the delay epoch. We asked whether this activity profile of gamma could be linked with the sensory-motor integration processes (23, 24), especially because of its timing and spatial tuning properties. Because the neurons that were recorded simultaneously with the LFP also showed spatial tuning in both visual and saccadic epochs, we asked whether the gamma tuning was correlated with either of these neuronal tuning properties. Hence, we plotted the Spearman rho values of pairwise correlations between the saccade tuning and gamma tuning (ordinate) against the pairwise correlations of visual tuning and gamma tuning (abscissa), for each neuron. We found that the gamma activity's tuning was more similar to the saccade tuning than the visual tuning of the neurons (Fig. 7*E*). To account for the possibility that the neural firing in the delay period might have an influence on the gamma activity, we also calculated the spike

tuning in the memory epoch and correlated that with the gamma activity and found that none of the pairs were significantly correlated (spearman correlation; *P* > 0.05; Fig. S3*A*). Taken together, these results suggest that gamma activity could reflect the sensory to motor transformation.

To test this hypothesis further, we asked if gamma in FEF could predict the saccadic reaction times (RTs) of the animal. We calculated a trial-by-trial average of gamma activity in the delay period and estimated the RT as the time of the saccade onset from the "go" signal. We then classified the RT into four quantiles, and we took the first quantile as the "fast" group and the last quantile as the "slow" group to see the effects in the extreme ends. We also binned the average gamma activity based on these two RT groups. We found that the gamma in the delay period could predict the RT, with the effect being stronger in the RF positions (Fig. 7*F*; RF fast: 0.79 ± 0.05, RF slow: 0.47 ± 0.06; *n* = 58, *P* < 10^{-54}; aRF fast: 0.51 ± 0.06, aRF slow: 0.40 ± 0.06; *P* < 10^{-14}), but the spiking activity in the same epoch couldn't (RF, *P* = 0.8375, aRF, *P* = 0.3032; Fig. S3*B*).

Characterization of Beta Band Activity in FEF. Beta band decreased in activity in the saccadic epoch (Fig. 6*A*, *Right*) with no spatial tuning (Fig. 6*B*, *Right*). Fig. 8*A* shows the average activity in the beta band for one representative LFP site averaged across all spatial positions. Unlike gamma activity, beta activity did not show any modulation in activity during the delay epoch but started to show a suppression in activity in the presaccadic epoch and attained a minima close to the saccade execution time.

The beta activity in the visual (−0.02 ± 0.06) and the delay epochs (−0.25 ± 0.08) weren't significantly different from each other (*n* = 58; *P* = 0.0672). However, the beta activity decreased significantly during the saccadic epoch (−0.82 ± 0.07) from the delay epoch (*n* = 58, *P* < 10^{-6}). Furthermore, the baseline beta power (0.07 ± 0.05) was not significantly different from the visual epoch (*P* = 0.2192) but was significantly different from the saccadic epoch (*P* < 10^{-13}). Therefore, beta showed suppression in activity only during the saccadic epoch (Fig. 8*B*). Also, the time of maximum beta suppression was 24.9 ± 20.0 ms after the saccade. This suppression of beta activity was not spatially tuned (Fig. 8*C*) and did not correlate with RT (fast: −1.59 ± 0.12, slow: −1.62 ± 0.11; *n* = 58, *P* = 0.9791;
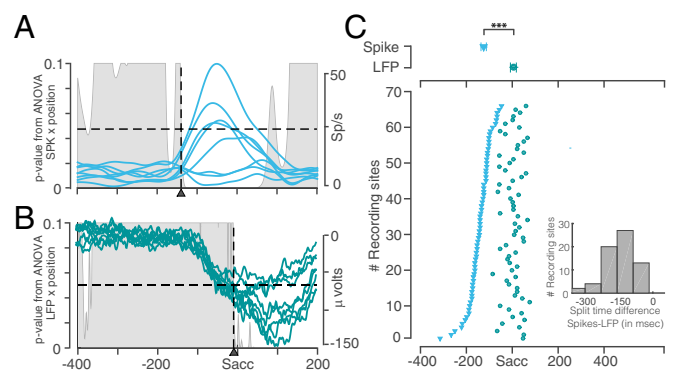

Fig. 4. Saccade plan specification times for spikes and LFP. (*A*) SPS for a representative neuron. The average spike density function in each of the eight positions for the representative neuron (solid lines) superimposed on the *P* value obtained from ANOVA across the signals from eight positions, indicating the probability that the signals were not different from each other (gray shaded region). The SPS for this neuron was −141 ms (vertical dashed line). (*B*) SPS for the simultaneously recorded LFP signal. Same format as above. The SPS$_{LFP}$ for this site was −2 ms (vertical dashed line). (*C*) *Bottom* shows the SPS$_{SPK}$ (blue triangles) and SPS$_{LFP}$ (green circles) for all sessions sorted by SPS$_{SPK}$ times. *Upper* shows the mean SPS$_{SPK}$ SPS$_{LFP}$; *t* test, *P* < 10^{-22}. *Inset* shows the distribution of ΔSPS between each SPK-LFP pair.
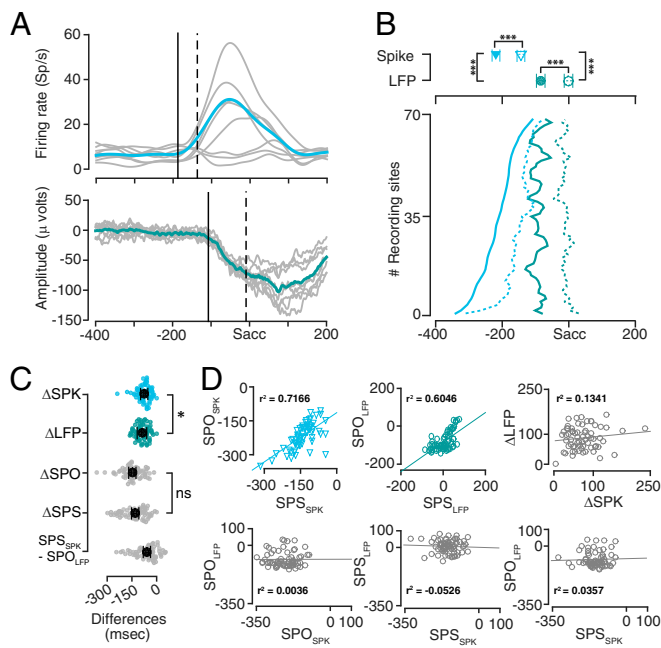
Sendhilnathan et al.

www.manaraa.com

Fig. 5. Comparison of saccade plan onset and specification times for spikes and LFP. (*A, Top*) The average firing rate from a representative neuron in each of the eight positions (gray) superimposed with the average firing rate across all eight positions (green). SPO is shown as a solid line, and the SPS is shown as a dashed line. (*A, Lower*) Same format as *Upper*, but for LFP from a representative site. All traces were taken from Figs. 3 and 4. (*B*) The SPO (solid lines) and SPS (dashed lines) for LFP (green) and spikes (blue) for all of the sessions, sorted by SPO$_{SPK}$. The plot is smoothened for ease of viewing. *Upper* shows the mean and SEM for the SPO and SPS for LFP and spikes. All traces were taken from Figs. 3 and 4. (*C*) Pairwise differences between the SPO$_{SPK}$ and SPS$_{SPK}$ (ΔSPK), SPO$_{LFP}$ and SPS$_{LFP}$ (ΔLFP). Pairwise differences between the SPO$_{LFP}$ and SPO$_{SPK}$ (ΔSPO) and the SPS$_{LFP}$ and SPS$_{SPK}$ (ΔSPS). Difference between SPO$_{LFP}$ and SPS$_{SPK}$. The mean and the SEs are shown as superimposed black markers. (*D*) The SPO and SPS were well correlated within spike and LFP, but not across spike and LFP. *Upper Left*, scatter plot between the SPS$_{SPK}$ (abscissa) and SPO$_{SPK}$ (ordinate). Regression line is shown as a solid blue line. *Upper Middle*, similarly for LFP. *Upper Right*, time lag between SPO and SPS was not correlated between spikes and LFP. *Lower*, same format as above, but for SPO$_{LFP}$ vs. SPO$_{SPK}$ onset (*Left*); SPS$_{LFP}$ vs. SPS$_{SPK}$ (*Middle*); SPO$_{LFP}$ vs. SPS$_{SPK}$ (*Right*).

Fig. 8*D*). Although beta activity showed a distinct modulation in activity during the saccade preparation epoch, it lacked spatial tuning, did not predict the RT, and was temporally proximal to the saccade onset.

Discussion

By comparing the time course and frequency components of the LFP relative to spiking activity of FEF neurons, we report two main findings. First, the LFP showed visually evoked responses significantly earlier than the spikes (Fig. S1), but the spikes had information about the planned saccade (Fig. 3) and its direction (Fig. 4) significantly earlier than the LFP (Fig. 5). Second, gamma activity showed elevated activity with spatial selectivity in the delay epoch, after the visual stimulus presentation and well before the saccade epoch, with a tuning more similar to the neural saccadic tuning than the visual tuning. Gamma activity also predicted the RT, suggesting that it represents an important aspect of the local computation that represents the visuomotor transformation occurring within FEF (Fig. 7). In contrast, beta activity showed a nondirectionally selective suppression in activity just before saccade initiation (Fig. 8). Here, we discuss some important implications of our results.

Input Characteristics of FEF. The VRL that we report is in agreement with the previously reported values by other groups (ref. 1; LFP, early: 51.7 ± 0.5 ms, late: 61.5 ± 0.8 ms; spike, early: 65.0 ± 3.3 ms, late: 79.0 ± 2.9 ms. Ref. 28; LFP: 56.5 ms and spike: 68.5 ms). We report a VRL of 58.9 ± 1.65 ms in LFP and 78.43 ± 1.16 ms in spikes (Table S1), which suggests that the LFP has information regarding the location of the visual stimulus significantly earlier than the spikes in FEF, supporting previous studies (1, 28).

The Role of FEF in Saccade Planning. In this study, we show that although the LFP in FEF had an earlier visually evoked response in the saccade epoch, the spiking activity of FEF neurons possessed information about the planning of saccade and its direction earlier than the LFP by ~130 ms for SPO and ~145 ms for SPS across the two monkeys (Table S1). This reported relationship between LFP and spikes was not affected by the potential effects due to LFP or spike filtering (*SI Materials and Methods* and Fig. S4). Interestingly, saccade selectivity in LFP developed within a temporally narrow epoch, very close to the saccade execution time. Hence, if we interpret LFP selectivity to represent input and spiking selectivity to represent output, we infer that FEF generates saccade plans internally and may represent the first step where the critical visuomotor transformation occurs. We report markers for two phases of saccadic computation: SPO time, when the global plan for a saccade is initiated, and SPS time, when the direction of the saccade being planned is selected. We further showed that the relationship between spikes and LFP was similar in both these phases of computation.

In this context, it is interesting to note that prior studies have shown that the lateral intraparietal area (LIP), which provides prominent input to FEF and also possess cells with visuomotor properties, shows the converse relation between LFP and spiking activity, where LFP has earlier and more robust information regarding the planning and execution of saccades than the spikes (21). These evidences taken together suggest that saccade plans are generated in FEF internally and relayed to LIP through their reciprocal feedback connections. These results are consistent with the notion that LIP is primarily a visual area playing an active role in visual selection but a more passive role in the visuomotor transformation process. Consistent with this interpretation, saccade countermanding or active online cancellation of saccades is readily observed in the activity of movement-related cells in the FEF but not in LIP (29).

If the SPS$_{SPK}$ time represents an intrinsic visuomotor transformation occurring within FEF, then what does the ensuing SPS$_{LFP}$ reflect? Because electrical stimulation of FEF requires at least 30–45 ms to elicit a saccade (30), one can assume that a signal, in FEF, showing a SPO or SPS less than 30–45 ms before saccade might not play a potential role in saccade generation. In this study, we report a SPO$_{LFP}$ of −84.4 ± 5.6 ms and a SPS$_{LFP}$ of 3.2 ± 4.7 ms relative to saccade onset, supporting our argument
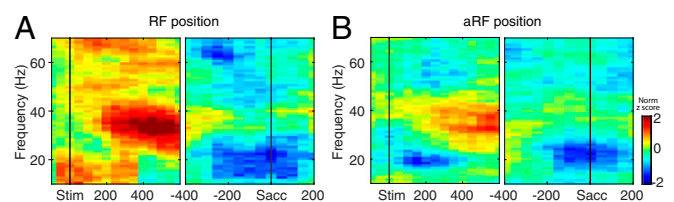

Fig. 6. Time-frequency spectrogram for a representative LFP site. (*A*) Time-frequency spectrogram for the RF position aligned to stimulus onset (*Left*) and saccade onset (*Right*) showing an increase in gamma (30–70 Hz) power in the delay epoch and a decrease in beta (13–30 Hz) power before saccade. (*B*) Same format as *A* above, but for aRF, showing a low level of gamma increase and no change in beta decrease.

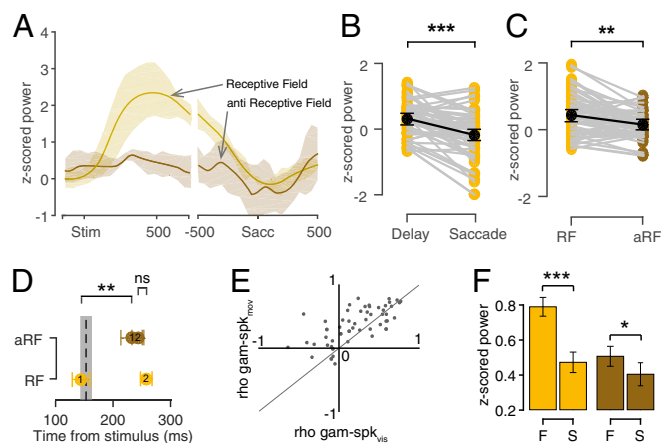Sendhilnathan et al.

www.manaraa.com

Fig. 7. Gamma band properties. (*A*) z-scored gamma power of a representative LFP site for RF (yellow) and aRF (brown) positions, aligned to stimulus onset (*Left*) and saccade onset (*Right*). Shading, standard deviation. (*B*) The average peak z-scored gamma power for the population of recorded LFP sites in the delay epoch, 150–350 ms after the visual stimulus presentation and in the saccade epoch, −300 to 100 ms from saccade onset; *t* test $P < 10^{-5}$. (*C*) The average peak z-scored gamma power for the population of recorded LFP sites in the memory period in the RF (yellow) and aRF (brown). (*D*) Onset time for gamma power in RF (1, yellow) and in aRF (1, brown). The dotted line shows the first time when the gamma power in RF significantly differed from the gamma power in aRF position. Peak time for gamma power in RF (2, yellow) in aRF (2, brown). (*E*) A scatter plot between the r^2 values obtained from correlating gamma tuning with visual tuning of spikes (*x* axis) and correlating gamma tuning with the saccadic tuning of spikes (*y* axis) showing that gamma tuning is more linked with saccade tuning. The thin solid line is the line of unity. (*F*) Gamma activity in the RF (*Left*) and the aRF (*Right*) positions for fast (F) and slow (S) RTs.

that the LFP in FEF might not be contributing to saccade preparation per se. However, it is known that FEF receives a saccade-related input from medial dorsal nucleus ∼96 ms before a saccade, which is thought to be a corollary discharge of the impending saccade plan from the superior colliculus (31, 32). A consequence of this corollary discharge is the shift of RF by FEF neurons before the onset of a saccade. FEF neurons shift their RF in a range from 100 ms before to 200 ms after the saccade initiation, with the average being ∼24 ms after saccade initiation (32). Thus, conforming to the idea that LFP might represent the synaptic input, one might expect LFP in the saccade epoch to represent this input information. The values we report for LFP in this study are in agreement with those results. More interestingly, we find a narrow range of SPO_{LFP} and SPS_{LFP} range that were not correlated with the spike counterparts, suggesting different origins of these two signals. Thus, our data raise the intriguing hypothesis that aspects of LFP might reflect this corollary discharge that FEF receives just before a saccade.

Gamma Band Activity Reflects the Visuomotor Transformation. Previous studies in LIP have shown that in the delay epoch, a spatially tuned elevation in activity in the gamma band (30–70 Hz) might contribute to the maintenance of "memory fields," which are important in working memory (21), whereas other studies have suggested that gamma activity could be involved in the sensory-motor integration process (23, 24). Our results indicate that these two roles might not be mutually exclusive. The gamma activity raised in power in a time frame that was much later than the initial visual response period in sensory-motor regions including FEF (33) and LIP (21) but also much earlier than the saccade epoch and, therefore, may represent an important intermediate step of visual selection that precedes saccades.

Visual selection is an important component of the visuomotor transformation process, necessary for planning of relevant saccades. It is also considered as the link between perceptual processes and action or execution (34). Monosov et al. showed that FEF neurons have visual selection times (105–133 ms) significantly earlier than the LFP (134–152 ms) and that the FEF neurons were the functionally active units that performed this computation from their visual input (LFP) from other brain regions. Hence, the later selection time noted in the LFP could be a reflection of local computation in FEF. Because we used a memory-guided saccade task in our study, it did not involve classical target selection due to the absence of distractors. Nevertheless, the time of gamma increase we report might be a signature of this covert visual attention process and goal selection for the upcoming saccade.

Whereas the spatial selectivity of gamma activity during the delay period (23, 24) implies a role in working memory of stimulus location, it is typically thought to reflect sensory memory, and like visual selection, is not expected to be correlated with RT (36). However, consistent with previous work, we showed that gamma activity, but not the corresponding spiking activity, was correlated with RT (23, 24). Additionally, the gamma activity in the delay epoch was more closely tuned to the saccadic tuning than the visual tuning of the cell. These results suggest that gamma oscillations may reflect intracortical processing within FEF that aids in transformation of sensory information into a saccade plan.

Beta Activity Represents Undifferentiated Neural Activity. Beta suppression has been considered as an "undifferentiated reflection of neural activity" (26) because the amplitude of suppression is not clearly modulated by motor parameters like direction (36), speed (26), or duration (37). However, in oculomotor regions, it gets modulated in an epoch close to the initiation of the saccade but the modulation characteristics itself might differ between different cortical regions, from being a spatially invariant suppression of activity in regions like LIP before a saccade (21, 38) or a spatially selective elevation of activity in regions like the posterior parietal cortex before a coordinated reach and saccade (39). We investigated beta modulation in the FEF and characterized the properties of beta band activity in the visual, delay, and the saccadic epochs to check for any functional significance during the visuomotor transformation process.

In contrast to gamma activity, beta band activity was not spatially tuned and showed a suppression in activity close to saccade onset but did not correlate with RT. Because the beta band activity represented a gradual suppression in power, starting before the eye movement and was just not a transient
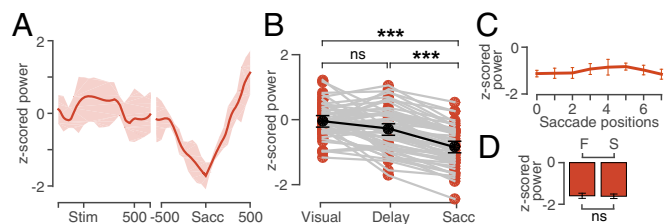

Fig. 8. Beta band properties. (*A*) Average z-scored beta power aligned to stimulus onset (*Left*) and saccade onset (*Right*) showing a decrease in beta power below the baseline level, during the saccade epoch. Shading: standard deviation (*B*) The average peak z-scored beta power for the population of recorded LFP sites in the visual epoch, delay epoch, and the saccade epoch. (*C*) The average z-scored beta power in all eight positions for the population of recorded LFP sites in the saccade epoch showing no significant tuning. (*D*) Population average beta activity for fast (F) and slow (S) RTs.

Sendhilnathan et al.

www.manaraa.com

phenomenon revealed solely at the time of saccade execution, we believe that it is unlikely to reflect an EOG signal artifact. Additionally, beta band power started to differ from baseline at a time point later than the saccade specification time of FEF and is therefore unlikely to reflect a direct role in saccade specification, similar to what has been shown in LIP (21, 38). Recent evidence however suggests that beta activity might be a reflection of motor preparation (40) and may be involved in other aspects of motor preparation such as eye-hand coordination (39) or a corollary discharge signal.

Materials and Methods

Two adult monkeys, J (male, *Macaca radiata*) and G (female, *Macaca mullata*) were used for the experiments. They were cared for in accordance with the Committee for the Purpose of Control and Supervision of Experiments of Animals, Government of India. Full details on the task design, physiology, and analysis can be found in the *SI Materials and Methods*.

1. Monosov IE, Trageser JC, Thompson KG (2008) Measurements of simultaneously recorded spiking activity and local field potentials suggest that spatial selection emerges in the frontal eye field. *Neuron* 57:614–625.
2. Thompson KG, Biscoe KL, Sato TR (2005) Neuronal basis of covert spatial attention in the frontal eye field. *J Neurosci* 25:9479–9487.
3. Bushnell MC, Goldberg ME, Robinson DL (1981) Behavioral enhancement of visual responses in monkey cerebral cortex. I. Modulation in posterior parietal cortex related to selective visual attention. *J Neurophysiol* 46:755–772.
4. Bruce CJ, Goldberg ME (1985) Primate frontal eye fields. I. Single neurons discharging before saccades. *J Neurophysiol* 53:603–635.
5. Purcell BA, Schall JD, Woodman GF (2013) On the origin of event-related potentials indexing covert attentional selection during visual search: Timing of selection by macaque frontal eye field and event-related potentials during pop-out search. *J Neurophysiol* 109:557–569.
6. Schall JD (1991) Neuronal activity related to visually guided saccades in the frontal eye fields of rhesus monkeys: Comparison with supplementary eye fields. *J Neurophysiol* 66:559–579.
7. Duhamel JR, Colby CL, Goldberg ME (1992) The updating of the representation of visual space in parietal cortex by intended eye movements. *Science* 255:90–92.
8. Schall JD (1991) Neuronal activity related to visually guided saccadic eye movements in the supplementary motor area of rhesus monkeys. *J Neurophysiol* 66:530–558.
9. Wurtz RH, Goldberg ME (1972) Activity of superior colliculus in behaving monkey. 3. Cells discharging before eye movements. *J Neurophysiol* 35:575–586.
10. Kim J-N, Shadlen MN (1999) Neural correlates of a decision in the dorsolateral prefrontal cortex of the macaque. *Nat Neurosci* 2:176–185.
11. Mitzdorf U (1985) Current source-density method and application in cat cerebral cortex: Investigation of evoked potentials and EEG phenomena. *Physiol Rev* 65:37–100.
12. Chen C-M, et al. (2007) Functional anatomy and interaction of fast and slow visual pathways in macaque monkeys. *Cereb Cortex* 17:1561–1569.
13. Buzsáki G, Anastassiou CA, Koch C (2012) The origin of extracellular fields and currents–EEG, ECoG, LFP and spikes. *Nat Rev Neurosci* 13:407–420.
14. Buzsáki G (2006) *Rhythms of the Brain* (Oxford Univ Press, Oxford).
15. Khawaja FA, Tsui JMG, Pack CC (2009) Pattern motion selectivity of spiking outputs and local field potentials in macaque visual cortex. *J Neurosci* 29:13702–13709.
16. Cohen JY, Heitz RP, Schall JD, Woodman GF (2009) On the origin of event-related potentials indexing covert attentional selection during visual search. *J Neurophysiol* 102:2375–2386.
17. Fries P, Reynolds JH, Rorie AE, Desimone R (2001) Modulation of oscillatory neuronal synchronization by selective visual attention. *Science* 291:1560–1563.
18. Womelsdorf T, et al. (2007) Modulation of neuronal interactions through neuronal synchronization. *Science* 316:1609–1612.
19. Gregoriou GG, Gotts SJ, Zhou H, Desimone R (2009) High-frequency, long-range coupling between prefrontal and visual cortex during attention. *Science* 324:1207–1210.
20. Melloni L, et al. (2007) Synchronization of neural activity across cortical areas correlates with conscious perception. *J Neurosci* 27:2858–2865.
21. Pesaran B, Pezaris JS, Sahani M, Mitra PP, Andersen RA (2002) Temporal structure in neuronal activity during working memory in macaque parietal cortex. *Nat Neurosci* 5:805–811.
22. Lundqvist M, et al. (2016) Gamma and beta bursts underlie working memory. *Neuron* 90:152–164.
23. Fründ I, Busch NA, Schadow J, Körner U, Herrmann CS (2007) From perception to action: Phase-locked gamma oscillations correlate with reaction times in a speeded response task. *BMC Neurosci* 8:27.
24. Ghuman AS, et al. (2014) Dynamic encoding of face information in the human fusiform gyrus. *Nat Commun* 5:5672.
25. Jasper H, Penfield W (1949) Electrocorticograms in man: Effect of voluntary movement upon the electrical activity of the precentral gyrus. *Arch Psychiatr Nervenkr* 183:163–174.
26. Stancák A, Jr, Pfurtscheller G (1996) Event-related desynchronisation of central beta-rhythms during brisk and slow self-paced finger movements of dominant and nondominant hand. *Brain Res Cogn Brain Res* 4:171–183.
27. Sochůrková D, Rektor I, Jurák P, Stancák A (2006) Intracerebral recording of cortical activity related to self-paced voluntary movements: A Bereitschaftspotential and event-related desynchronization/synchronization. SEEG study. *Exp Brain Res* 173:637–649.
28. Purcell BA, Heitz RP, Cohen JY, Schall JD (2012) Response variability of frontal eye field neurons modulates with sensory input and saccade preparation but not visual search salience. *J Neurophysiol* 108:2737–2750.
29. Paré M, Dorris MC (2011) The role of posterior parietal cortex in the regulation of saccadic eye movements. *The Oxford Handbook of Eye Movements*, 257–278.
30. Bruce CJ, Goldberg ME, Bushnell MC, Stanton GB (1985) Primate frontal eye fields. II. Physiological and anatomical correlates of electrically evoked eye movements. *J Neurophysiol* 54:714–734.
31. Sommer MA, Wurtz RH (2004) What the brain stem tells the frontal cortex. I. Oculomotor signals sent from superior colliculus to frontal eye field via mediodorsal thalamus. *J Neurophysiol* 91:1381–1402.
32. Sommer MA, Wurtz RH (2008) Brain circuits for the internal monitoring of movements. *Annu Rev Neurosci* 31:317–338.
33. Gregoriou GG, Gotts SJ, Desimone R (2012) Cell-type-specific synchronization of neural activity in FEF with V4 during attention. *Neuron* 73:581–594.
34. Serences JT, Yantis S (2006) Selective visual attention and perceptual coherence. *Trends Cogn Sci* 10:38–45.
35. Thompson KG, Bichot NP, Schall JD (1997) Dissociation of visual discrimination from saccade programming in macaque frontal eye field. *J Neurophysiol* 77:1046–1050.
36. Waldert S, et al. (2008) Hand movement direction decoded from MEG and EEG. *J Neurosci* 28:1000–1008.
37. Cassim F, et al. (2000) Brief and sustained movements: Differences in event-related (de)synchronization (ERD/ERS) patterns. *Clin Neurophysiol* 111:2032–2039.
38. Chen M, Wei L, Liu Y (2014) Motor preparation attenuates neural variability and beta-band LFP in parietal cortex. *Sci Rep* 4:6809.
39. Dean HL, Hagan MA, Pesaran B (2012) Only coherent spiking in posterior parietal cortex coordinates looking and reaching. *Neuron* 73:829–841.
40. Tzagarakis C, Ince NF, Leuthold AC, Pellizzer G (2010) Beta-band activity during motor planning reflects response uncertainty. *J Neurosci* 30:11270–11277.
41. van der Meer MAA, Redish AD (2011) Theta phase precession in rat ventral striatum links place and reward information. *J Neurosci* 31:2843–2854.
42. Terada S, Takahashi S (2013) Oscillatory interaction between amygdala and hippocampus coordinates behavioral modulation based on reward expectation. *Front Behav Neurosci* 7:177.
43. Fisher NI (1995) *Statistical Analysis of Circular Data* (Cambridge Univ Press, Cambridge, UK).
44. Bokil H, Andrews P, Kulkarni JE, Mehta S, Mitra PP (2010) Chronux: A platform for analyzing neural signals. *J Neurosci Methods* 192:146–151.
45. Thomson DJ (1982) Spectrum Estimation and Harmonic Analysis. *Proc IEEE* 70:1055–1096.

NEUROSCIENCE

Sendhilnathan et al.

www.manaraa.com